Journal of Pathology
J Pathol 2016; **239:** 206–217
Published online 26 April 2016 in Wiley Online Library
(wileyonlinelibrary.com) DOI: 10.1002/path.4719

ORIGINAL PAPER

K-Ras^{V14I}-induced Noonan syndrome predisposes to tumour development in mice

Isabel Hernández-Porras,[1] Alberto J Schuhmacher,[1†] Raquel Garcia-Medina,[1] Beatriz Jiménez,[1] Marta Cañamero,[2‡] Alba de Martino[2] and Carmen Guerra[1,*]

[1] *Molecular Oncology, Centro Nacional de Investigaciones Oncológicas (CNIO), Madrid, Spain*
[2] *Biotechnology Programs, Centro Nacional de Investigaciones Oncológicas (CNIO), Madrid, Spain*

**Correspondence to: C Guerra, Centro Nacional de Investigaciones Oncológicas, Programa de Oncología Molecular, C/Melchor Fernandez Almagro 3, Madrid 28029, Spain. E-mail: mcguerra@cnio.es*

[†] *Present address: Cancer Cell Biology Program, CNIO, E-28029 Madrid, Spain.*
[‡] *Present address: Roche Pharmaceutical Research and Early Development, Translational Medicine Oncology, Innovation Center, 82377 Penzberg, Germany.*

Abstract

The Noonan syndrome (NS) is an autosomal dominant genetic disorder characterized by short stature, craniofacial dysmorphism, and congenital heart defects. A significant proportion of NS patients may also develop myeloproliferative disorders (MPDs), including juvenile myelomonocytic leukaemia (JMML). Surprisingly, scarce information is available in relation to other tumour types in these patients. We have previously developed and characterized a knock-in mouse model that carries one of the most frequent *KRAS*-NS-related mutations, the K-*Ras*^{V14I} substitution, which recapitulates most of the alterations described in NS patients, including MPDs. The K-*Ras*^{V14I} mutation is a mild activating K-Ras protein; thus, we have used this model to study tumour susceptibility in comparison with mice expressing the classical K-*Ras*^{G12V} oncogene. Interestingly, our studies have shown that these mice display a generalized tumour predisposition and not just MPDs. In fact, we have observed that the K-*Ras*^{V14I} mutation is capable of cooperating with the *p16Ink4a/p19Arf* and *Trp53* tumour suppressors, as well as with other risk factors such as pancreatitis, thereby leading to a higher cancer incidence. In conclusion, our results illustrate that the K-Ras^{V14I} activating protein is able to induce cancer, although at a much lower level than the classical K-*Ras*^{G12V} oncogene, and that it can be significantly modulated by both genetic and non-genetic events.
Copyright © 2016 Pathological Society of Great Britain and Ireland. Published by John Wiley & Sons, Ltd.

Keywords: K-Ras; RASopathies; Noonan syndrome; cancer

Received 27 October 2015; Revised 8 March 2016; Accepted 11 March 2016

No conflicts of interest were declared.

Introduction

The RAS/MAPK pathway is an essential pathway for embryo development, cell signalling, and proliferation [1,2]. Germline mutations in the *RAS* genes or in components or regulators of the RAS/MAPK pathway result in developmental disorders known as RASopathies that include the Noonan syndrome (NS), Costello syndrome (CS), and neurofibromatosis type 1 (NF1) [3]. NS is a relatively frequent developmental disorder mainly characterized by craniofacial dysmorphia, short stature, cardiovascular and skeletal defects, delayed puberty, and learning difficulties [1,3,4]. NS may result from germline mutations in 11 different loci (*PTPN11*, *SOS1*, *KRAS*, *NRAS*, *RAF1*, *BRAF*, *MEK1*, *SHOC2*, *CBL*, *RIT1*, and *RRAS*), which are not usually found in cancer [5–7]. However, the somatic *KRAS*^{V14I}-NS-associated mutation has been identified in some human tumours, mainly in intestinal tumours (COSMIC database).

Misregulation of the RAS/MAPK pathway has been previously implicated in cancer biology [1,2]. *RAS* somatic missense mutations are found in about 30% of human cancers. *KRAS* is the most frequent mutated oncogene in pancreatic (90%), colon (50%), and lung tumours (25%). Furthermore, it is the initiating oncogenic event in lung and pancreatic cancers [1,8]. Thus, deregulation of this pathway during embryo development could lead to an increased tumour predisposition. Indeed, this is the situation for CS and NF1 [9,10]. Moreover, about 10% of NS patients exhibit transient MPDs. Less frequently, these patients develop severe MPDs, juvenile myelomonocytic leukaemia (JMML), and/or other haematological malignancies [11]. In spite of the high number of NS patients and their potential tumour predisposition, only four studies have described haematopoietic malignancies as the most frequent tumours, followed by rhabdomyosarcoma, neuroblastoma, central nervous system tumours, scarce

Copyright © 2016 Pathological Society of Great Britain and Ireland.
Published by John Wiley & Sons, Ltd. www.pathsoc.org

angiosarcomas, colon cancer, and basal cell carcinoma [11–14]. A review of 1151 NS patients with unknown mutations identified 3.9% of cancer cases. This study showed a cumulative cancer incidence of 4% by the age of 20, which is still lower than the 15% for CS [13]. Furthermore, a cohort study of 297 young NS patients with *PTPN11* mutations provided a cumulative risk for developing cancer of 23% at the age of 55, which represents a 3.5-fold increased risk compared with the general population [11]. Recently, a population-based study identified an 8.1-fold increased cancer risk in NS children with *PTPN11*, *NRAS*, *SOS1*, and *RAF1* germline mutations. Interestingly, infants with *KRAS* germline mutations displayed a 75.8-fold increased risk [14]. These results suggest that germline mutations in genes of the RAS/MAPK pathway are associated with a significantly higher cancer risk.

We have generated a mouse model that expresses one of the most frequent NS-associated germline *KRAS* mutations, the K-*Ras*^{V14I} mutation, which recapitulates most of the alterations described in NS patients [15]. We used these mice to study the tumour predisposition associated with the expression of this mutation alone or in combination with non-genetic risk factors such as pancreatitis, as well as with the loss of tumour suppressor genes. Interestingly, the K-*Ras*^{V14I} mice had an overall increased tumour predisposition, not just MPDs, which cooperated with both pancreatitis and the loss of *p16Ink4a/p19Arf* and *Trp53* tumour suppressor genes. Hence, human epidemiological studies should be conducted in order to unveil the real impact of *KRAS*-NS-associated mutations in tumour development. Further studies should analyse other *KRAS* mutations, additional risk factors, and the cooperation with other genetic events. Our model could help to challenge tumour development and test new therapies aimed at preventing or treating cancer.

Materials and methods

Mice

Animal use was approved by the Ethical Committee of the Spanish National Cancer Research Center. The strains used were K-*Ras*$^{+/LSLV14I}$ and K-*Ras*^{V14I} [15], *RERT* [16], *Elas-tTA/tetO*-Cre [17], *p16Ink4a/p19Arf*$^{-/-}$ [18], *Trp53*$^{-/-}$ [19], and K-*Ras*$^{+/-}$ (unpublished data). Pancreatitis was induced by i.p. injection of caerulein for 6 months (125 µg/kg, 5 days/week; Sigma, St Louis, MO, USA) [17]. Tamoxifen treatment was performed by *ad libitum* administration of a tamoxifen-containing diet (Tekland68 CRD Tam^{400}/CreER). Infection with adeno-Cre particles (3×10^8 PFU/mouse) was performed in 8-week-old mice via intratracheal instillation after anaesthesia (ketamine 75 mg/kg, xylaxine 12 mg/kg, i.p.) [20]. Blood extraction from the renal vein was performed at necropsy. Blood populations were quantified using a blood analyser (Abacus Junior Vet; Diatron, Budapest, Hungary).

Histopathology and immunohistochemistry

Specimens were fixed in 10% buffered formalin, embedded in paraffin, serially sectioned (3 µm), and every tenth section was stained with H&E. Rehydrated sections were incubated with a primary antibody: (goat polyclonal anti-CD3 (1:250; 1127; Santa Cruz Biotechnology, Santa Cruz, CA, USA), rabbit polyclonal anti-CD31 (1:50; ab28364; Abcam antibodies, Cambridge, UK), rat monoclonal anti-F4/80 (1:10; Monoclonal Antibodies CNIO core unit; CNIO, Madrid, Spain), pre-diluted rabbit monoclonal Ki67 (SP6; 000311OQD; Master Diagnóstica, Granada, Spain), and goat polyclonal anti-Pax5 (1:500; 1974;Santa Cruz Biotechnolgy, Heidelberg, Germany), and then with the corresponding secondary antibody (rabbit anti-goat; Dako, Sant Just Desvern, Spain); and rabbit anti-rat; Vector Labs, Burlingame, CA, USA) and visualization systems as needed (OmniRabbit, Ventana; Roche Diagnostics, Sant Cugat del VallésSpain) conjugated with horseradish peroxidase. Immunohistochemical reactions were developed using 3,3'-diaminobenzidine tetrahydrochloride (DAB) as a chromogen (Chromomap DAB, Ventana, Roche or DAB solution, Dako) and nuclei were counterstained with Carazzi's haematoxylin. Finally, the slides were dehydrated, cleared, and mounted with a permanent mounting medium for microscopic evaluation.

Laser capture microdissection (LCM) and loss of heterozygosity (LOH) analysis

LCM (PALM microbeam Zeiss Axio Observer; Carl Zeiss, Jena, Germany) was used to isolate 10 000 cells from H&E-stained sections (3 µm) of tumours from K-*Ras*$^{+/V14I}$ mice. DNA was amplified by PCR with the following primers: forward (5IO_2: 5'-TACCGCAAGGGTAGGTGTTGG-3' and reverse (3Ex1_2: 5'-ACCAGCTCCAACCACCACAAG-3'), with a denaturing step of 94 °C at 5 min followed by 55 cycles of 60 s at 94 °C, 60 s at 60 °C, 60 s at 72 °C, and a final elongation step at 72 °C for 10 min. The PCR products were analysed by agarose gel electrophoresis, resulting in 403 and 669 bp fragments for the wild-type and the K-*Ras*^{V14I} allele, respectively.

Statistical analyses and data presentation

Data are presented as their means and respective standard errors (SEM) or as statistical scatter plots generated with Microsoft Excel, GraphPad Prism, and GraphPad calculator. The log-rank (Mantel–Cox) test was used to obtain p values when comparing survival curves. Mice were scored based on their highest-grade lesion and Fisher's exact test was used for histological tumour grading. $p < 0.05$ was considered statistically significant.

Copyright © 2016 Pathological Society of Great Britain and Ireland.
Published by John Wiley & Sons, Ltd. www.pathsoc.org

10969896, 2016, 2, Downloaded from https://pathsocjournals.onlinelibrary.wiley.com/doi/10.1002/path.4719 by Fundacion Del Sector Publico, Wiley Online Library on [19/06/2024]. See the Terms and Conditions (https://onlinelibrary.wiley.com/terms-and-conditions) on Wiley Online Library for rules of use; OA articles are governed by the applicable Creative Commons License

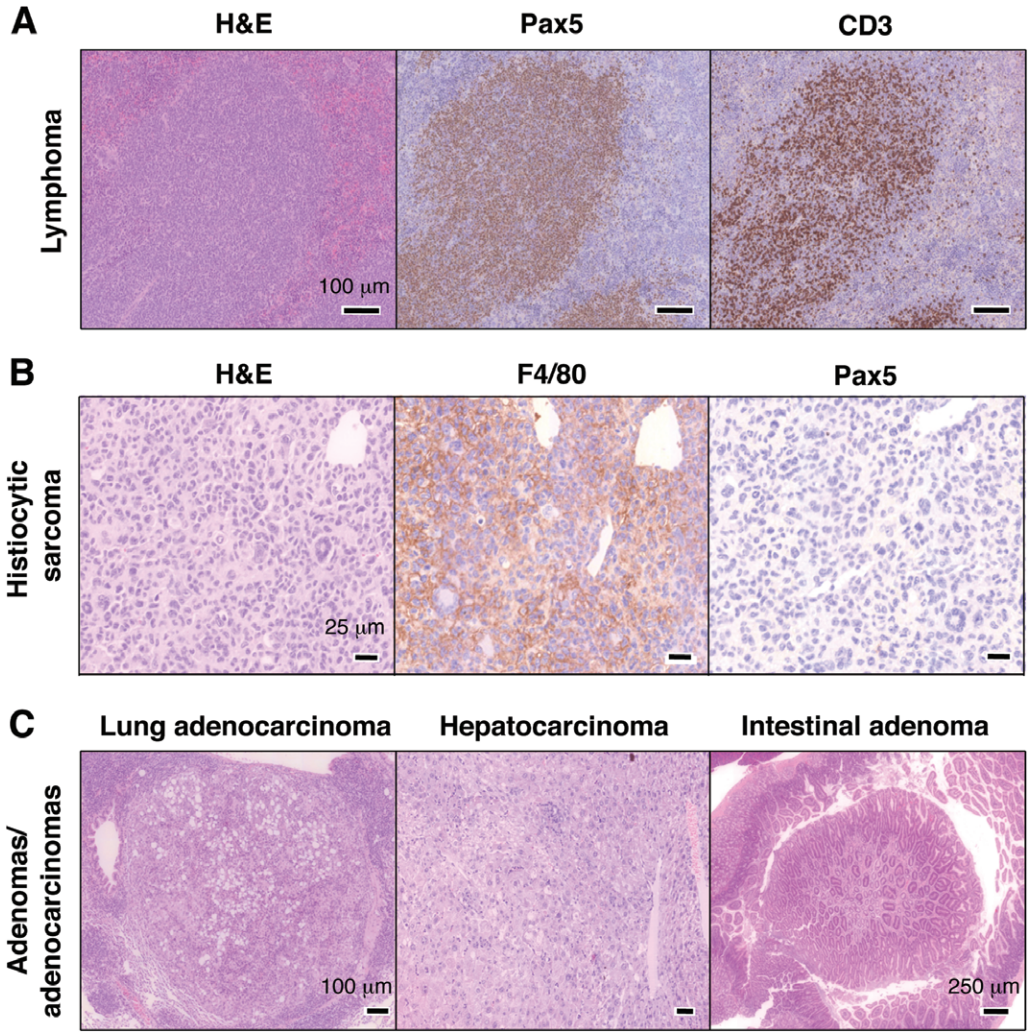

Figure 1. B6/129-K-*Ras*^{V14I} mice develop histiocytic sarcomas, lymphomas, and adenomas. (A) H&E-stained paraffin section and Pax5 and CD3 immunostaining of a representative lymphoma from K-*Ras*^{V14I} mice. (B) H&E-stained paraffin section and F4/80 and Pax5 immunostaining of a representative histiocytic sarcoma from K-*Ras*^{V14I} mice. (C) H&E-stained paraffin section of a representative lung adenocarcinoma, hepatocarcinoma, and intestinal tubular adenoma from K-*Ras*^{V14I} mice.

Results

K-*Ras*^{V14I} mice develop multiple malignancies

We have previously described the reduced longevity of K-*Ras*$^{+/V14I}$ and K-*Ras*$^{V14I/V14I}$ (K-*Ras*^{V14I}) mice in a mixed C57BL6J/129S2Sv (B6/129) background (half-life of 62 and 36 weeks, respectively) [15]. We have now determined that this reduction is due not only to MPD, but also to the development of haematopoietic alterations such as splenomegaly, leucocytosis, and anaemia (Supplementary Table 1). Histological evaluation of K-*Ras*$^{+/V14I}$ ($n = 26$) and K-*Ras*^{V14I} mice ($n = 12$) sacrificed at humane endpoints revealed the presence of multiple malignancies such as lymphomas, histiocytic sarcomas, and carcinomas. Furthermore, two K-*Ras*$^{+/V14I}$ animals developed leukaemia (Supplementary Tables 1 and 2 and Figure 1). Tumour development was slightly more prevalent in K-*Ras*$^{+/V14I}$ (24/26; 92%) than in K-*Ras*^{V14I} mice (9/12; 75%), possibly due to their longer survival. Other pathologies included renal changes, vasculitis, and areas of heart infarction (Supplementary Tables 1 and 2 and Supplementary Figure 1). These alterations could be either due to the expression of the K-*Ras*^{V14I} mutation or a consequence of the haematological disorder since they were always associated.

Wild-type mice were either sacrificed at a humane endpoint ($n = 6$) or between 89 and 113 weeks, which corresponds to the latest humane endpoint of their mutant littermates ($n = 6$). As expected, K-*Ras*$^{+/+}$ wild-type mice displayed a significantly lower tumour incidence than mutant mice, regardless of the time point. Histological evaluation of wild-type mice revealed the presence of early (17%; 1/6 mice) and advanced tumours (50%; 3/6 mice) at the humane endpoint, with the most frequent malignancies being lymphomas and histiocytic sarcomas. Renal pathological changes were found in 3 out of 12 mice (Supplementary Table 3). These results indicate that K-*Ras*^{V14I} expression enhances tumour development. K-*Ras*^{V14I} mice develop a diverse spectrum of haematological disorders, which in combination

Copyright © 2016 Pathological Society of Great Britain and Ireland.
Published by John Wiley & Sons, Ltd. www.pathsoc.org

10969896, 2016, 2, Downloaded from https://pathsocjournals.onlinelibrary.wiley.com/doi/10.1002/path.4719 by Fundacion Del Sector Publico, Wiley Online Library on [19/06/2024]. See the Terms and Conditions (https://onlinelibrary.wiley.com/terms-and-conditions) on Wiley Online Library for rules of use; OA articles are governed by the applicable Creative Commons License

with MPDs triggers their death. Moreover, germline expression of the K-*Ras*^{V14I} mutation induces the development of some lung tumours that are typical of the somatic expression of K-*Ras* oncogenes [2].

We have previously described that the survival rate of K-*Ras*^{V14I} mice depends on the genetic background. K-*Ras*^{V14I} mice backcrossed onto a 129S2/SvPasCrl (129) background results in an increased lifespan. In contrast, no alterations in longevity have been found in a C57BL/6 J.OlaHsd (B6) background [21]. As in the B6/129 mixed genetic background, reduced lifespan was linked to splenomegaly and leucocytosis (Supplementary Tables 4 and 5). While B6-K-*Ras*^{V14I} mice preferentially developed lymphomas (71%) and histiocytic sarcomas (43%), histological analysis of 129-K-*Ras*^{V14I} mice revealed the presence of a severe multifocal perivascular mixed inflammatory reaction in 83% of K-*Ras*$^{+/V14I}$ and in 67% of K-*Ras*^{V14I} mice (Supplementary Tables 4 and 5). This inflammatory process was characterized by a concentric perivascular cuffing of neutrophils, plasma cells, lymphocytes, and occasional eosinophils mainly observed in kidney, liver, and lung medium-size arteries. Progressively, necrotizing arteritis was developed with media and adventitia destruction, followed by granulation tissue replacement (Supplementary Figure 2). Renal pathological changes were observed in 50% of 129-K-*Ras*$^{+/V14I}$ mice and in 67% of 129-K-*Ras*^{V14I} mice (Supplementary Tables 4 and 5). B6 and 129 wild-type littermates were analysed at similar ages of the mutant's humane endpoint. B6-wild-type mice ($n = 5$) displayed a lower haematological tumour incidence (1/5) and none of the 129-wild-type mice ($n = 3$) showed inflammatory alterations.

The inflammatory situation and the vasculitis observed in 129-K-*Ras*^{V14I} mice suggest the development of an autoimmune reaction. Further studies are needed to understand the nature of this phenomenon observed in 14% of NS patients [22]. Our results advocate that the kidney alterations and vasculitis found in B6/129 mice are a direct consequence of the expression of the K-*Ras*^{V14I} mutation linked to the 129 genetic background.

K-*Ras*^{V14I} has the potential to induce lung tumours

KRAS oncogenes are found in 25% of human lung adenocarcinomas [23]. Somatic expression of oncogenic K-*Ras*^{G12D} or K-*Ras*^{G12V} alleles induces the appearance of lung adenomas in mice [16,24–26].

Lung tumours were only observed in 2 out of 26 K-*Ras*$^{+/V14I}$ mice, but not in K-*Ras*^{V14I} mice, which might be related to their shorter longevity (Supplementary Tables 1 and 2). To study K-*Ras*^{V14I}-induced lung tumours discarding the problem of the early lethality, we used the conditional strain K-*Ras*$^{+/LSLV14I}$ [15] and the K-*Ras*$^{+/LSLG12Vgeo}$ mice [16] as controls. In order to induce the expression of the K-*Ras*^{V14I} allele, we followed two different strategies: first, we performed intratracheal infection of 2-month-old K-*Ras*$^{+/LSLV14I}$ mice with a Cre-recombinase-expressing adenovirus. However, K-*Ras*^{V14I} expression in adult lungs did not induce lesions at 18 months of age ($n = 12$) (Figure 2A), when all K-*Ras*$^{+/LSLG12Vgeo}$ mice were sacrificed due to breathing difficulties as a result of tumour burden (Figure 2B) [27]. Second, we crossed the K-*Ras*$^{+/LSLV14I}$ mice with a knock-in strain (*RERT*) that expresses a ubiquitous and inducible Cre-ERT2 recombinase [16]. This strategy allows K-*Ras*^{V14I} expression in all the tissues upon tamoxifen treatment. To this end, K-*Ras*$^{+/LSLV14I}$;*RERT* ($n = 7$), K-*Ras*$^{+/LSLG12Vgeo}$;*RERT* ($n = 5$), and K-*Ras*$^{+/+}$;*RERT* ($n = 4$) mice were exposed to tamoxifen for 3 months from weaning. K-*Ras*$^{+/LSLV14I}$;*RERT* mice ($n = 7$) survived for at least 16 months without any alteration. Histological analysis of K-*Ras*$^{+/LSLV14I}$;*RERT* ($n = 7$) and K-*Ras*$^{+/+}$;*RERT* ($n = 4$) mice sacrificed at 16 months of age revealed the absence of lesions in the lung (Figure 2C) or in any other organ (data not shown). As expected, K-*Ras*$^{+/LSLG12Vgeo}$;*RERT* ($n = 5$) mice had to be sacrificed before 1 year of age, due to multiple lung adenomas and adenocarcinomas [16] (Figure 2D).

Importantly, these observations indicate that although the postnatal expression of the K-*Ras*^{V14I} mutation does not have enough oncogenic capacity to induce lung tumours, its germline expression has the potential to induce lung tumour development at a low incidence.

K-*Ras*^{V14I}-induced pancreatic lesions in the context of pancreatitis

KRAS mutations have been found in 90% of human pancreatic ductal adenocarcinomas (PDACs) [28,29], one of the tumours with the worst prognosis [30]. Mouse models have illustrated that K-*Ras* oncogenes are the initiating oncogenic event [17,31,32]. However, we observed a PDAC in only one out of six 129-K-*Ras*^{V14I} mice (Supplementary Table 4). Chronic pancreatitis, an important risk factor for PDAC development [33,34], has been shown to cooperate with oncogenic K-*Ras* mutations to induce a high number of pancreatic intraepithelial neoplasias (PanINs) and PDACs [17,34]. Thus, we studied whether chronic pancreatitis may have increased this risk in K-*Ras*^{V14I} mice by treating 2-month-old mice with daily doses of caerulein for 6 months. As expected, wild-type littermates did not display PanIN lesions, neither just after caerulein treatment ($n = 3$) nor 3 months after treatment ($n = 4$) (Figures 3A, 3B and Supplementary Figures 3A, 3B). In contrast, treatment of K-*Ras*$^{+/V14I}$ ($n = 15$) and K-*Ras*^{V14I} ($n = 13$) mice led to the appearance of PanIN lesions in most animals, including PanIN3, a direct PDAC precursor [35]. Just after caerulein treatment, 62% of K-*Ras*$^{+/V14I}$ mice and 87% of K-*Ras*^{V14I} mice displayed low-grade (LG) PanIN lesions. Moreover, 37% of K-*Ras*$^{+/V14I}$ mice and 87% of K-*Ras*^{V14I} mice developed high-grade (HG) PanIN2 and PanIN3 lesions (Supplementary Figure 3), yet no bona fide PDAC tumours were identified in K-*Ras*^{V14I} mice. Three months after treatment, only one out of seven K-*Ras*$^{+/V14I}$ mice displayed LG and HG

Copyright © 2016 Pathological Society of Great Britain and Ireland.
Published by John Wiley & Sons, Ltd. www.pathsoc.org

10969896, 2016, 2, Downloaded from https://pathsocjournals.onlinelibrary.wiley.com/doi/10.1002/path.4719 by Fundacion Del Sector Publico, Wiley Online Library on [19/06/2024]. See the Terms and Conditions (https://onlinelibrary.wiley.com/terms-and-conditions) on Wiley Online Library for rules of use; OA articles are governed by the applicable Creative Commons License

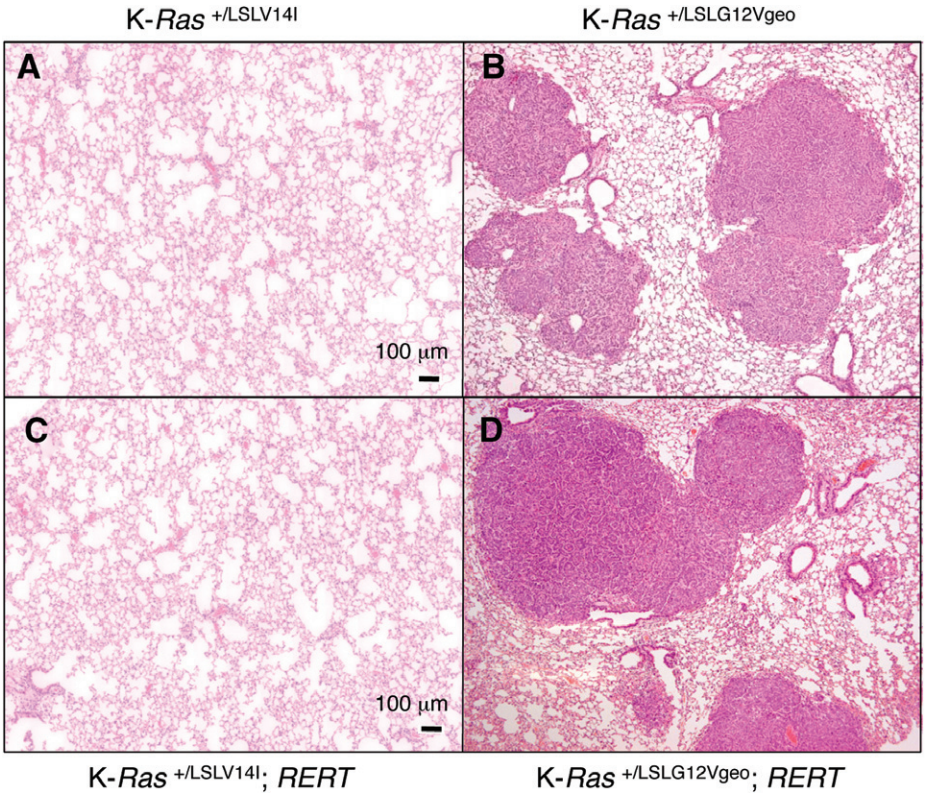

Figure 2. Expression of the K-*Ras*^{V14I} mutation in lung does not induce tumour development. (A) H&E-stained paraffin section of the lung of 18-month-old K-*Ras*$^{+/LSLV14I}$ mice infected intratracheally with adeno-Cre at 2 months of age. (B) H&E-stained paraffin section of the lung of 10-month-old K-*Ras*$^{+/LSLG12Vgeo}$ mice infected intratracheally with adeno-Cre at 2 months of age. (C) H&E-stained paraffin section of the lung of 16-month-old K-*Ras*$^{+/LSLV14I}$;*RERT* mice exposed to a tamoxifen diet for 3 months, starting at weaning (P21). (D) H&E-stained paraffin section of the lung of 8-month-old K-*Ras*$^{+/LSLG12Vgeo}$;*RERT* mice exposed to a tamoxifen diet for 3 months, starting at weaning (P21).

PanINs and three out of five K-*Ras*^{V14I} mice displayed LG and HG lesions. Again, no bona fide PDAC tumours were identified at this time (Supplementary Figure 3). Although K-*Ras*^{V14I} mice displayed PanIN lesions in the context of pancreatitis, the number of lesions was much lower than in K-*Ras*$^{+/LSLG12Vgeo}$ mice (Figures 3A and 3B), which usually develop pan-lobular lesions [17].

As previously reported, caerulein treatment induces tissue remodelling at the level of the stroma and acinar atrophy in both wild-type and K-*Ras*^{G12V} mice [17]. Interestingly, K-*Ras*^{V14I} mice, and to a lesser extent K-*Ras*$^{+/V14I}$ mice, displayed an exacerbated response to caerulein treatment, characterized by more fibrosis, oedema, acinar cell atrophy, and metaplasia than the wild-type (Figure 3C). Hence, these results suggest that NS patients might be more affected by inflammation than the general population and that K-*Ras*^{V14I} mutation could also predispose to tumour development in combination with certain chronic pathologies.

Finally, in order to clarify if the low number of lesions was due to germline expression of the K-*Ras*^{V14I} mutation and to perform a comparative study with our K-*Ras*^{G12V} PDAC model [17], we generated conditional K-*Ras*$^{+/LSLV14I}$;*Elas-tTA/tetO*-Cre mice. The *Elas-tTA/tetO*-Cre Tet-off system achieves expression of genes in about 30% of acinar cells [17]. K-*Ras*$^{+/LSLV14I}$;*Elas*-tTA/*tetO*-Cre mice ($n = 19$) expressed the K-*Ras*^{V14I} mutation in acinar cells from embryonic day (E) 16.5. At 2 months, these mice were treated with caerulein for 6 months. Under these conditions, oncogenic K-*Ras*^{G12V} mice displayed multiple all-grade PanIN lesions and PDACs [17]. In contrast, just after caerulein treatment, K-*Ras*$^{+/LSLV14I}$;*Elas-tTA/tetO*-Cre mice only displayed 30% (3/10) LG lesions and 10% (1/10) HG lesions (Figure 4 and Supplementary Figure 3C). Furthermore, only one out of nine K-*Ras*$^{+/LSLV14I}$;*Elas-tTA/tetO*-Cre mice displayed HG lesions 6 months after treatment (Figure 4A).

These results suggest that acinar-cell-specific K-*Ras*^{V14I} expression induces a lower PanIN incidence than germline expression. Furthermore, they illustrate a substantial difference in the oncogenic potential of the K-*Ras*^{V14I} and K-*Ras*^{G12V} activating mutations in the pancreas. However, even though K-*Ras*^{V14I} expression induced a low number of lesions, its presence should be considered an increased risk for PDAC development since wild-type mice do not develop any PanIN lesions.

Cooperation with the loss of tumour suppressor genes

Next, we examined whether the K-*Ras*^{V14I} mutation cooperated with the loss of the

Copyright © 2016 Pathological Society of Great Britain and Ireland.
Published by John Wiley & Sons, Ltd. www.pathsoc.org

10969896, 2016, 2, Downloaded from https://pathsocjournals.onlinelibrary.wiley.com/doi/10.1002/path.4719 by Fundacion Del Sector Publico, Wiley Online Library on [19/06/2024]. See the Terms and Conditions (https://onlinelibrary.wiley.com/terms-and-conditions) on Wiley Online Library for rules of use; OA articles are governed by the applicable Creative Commons License

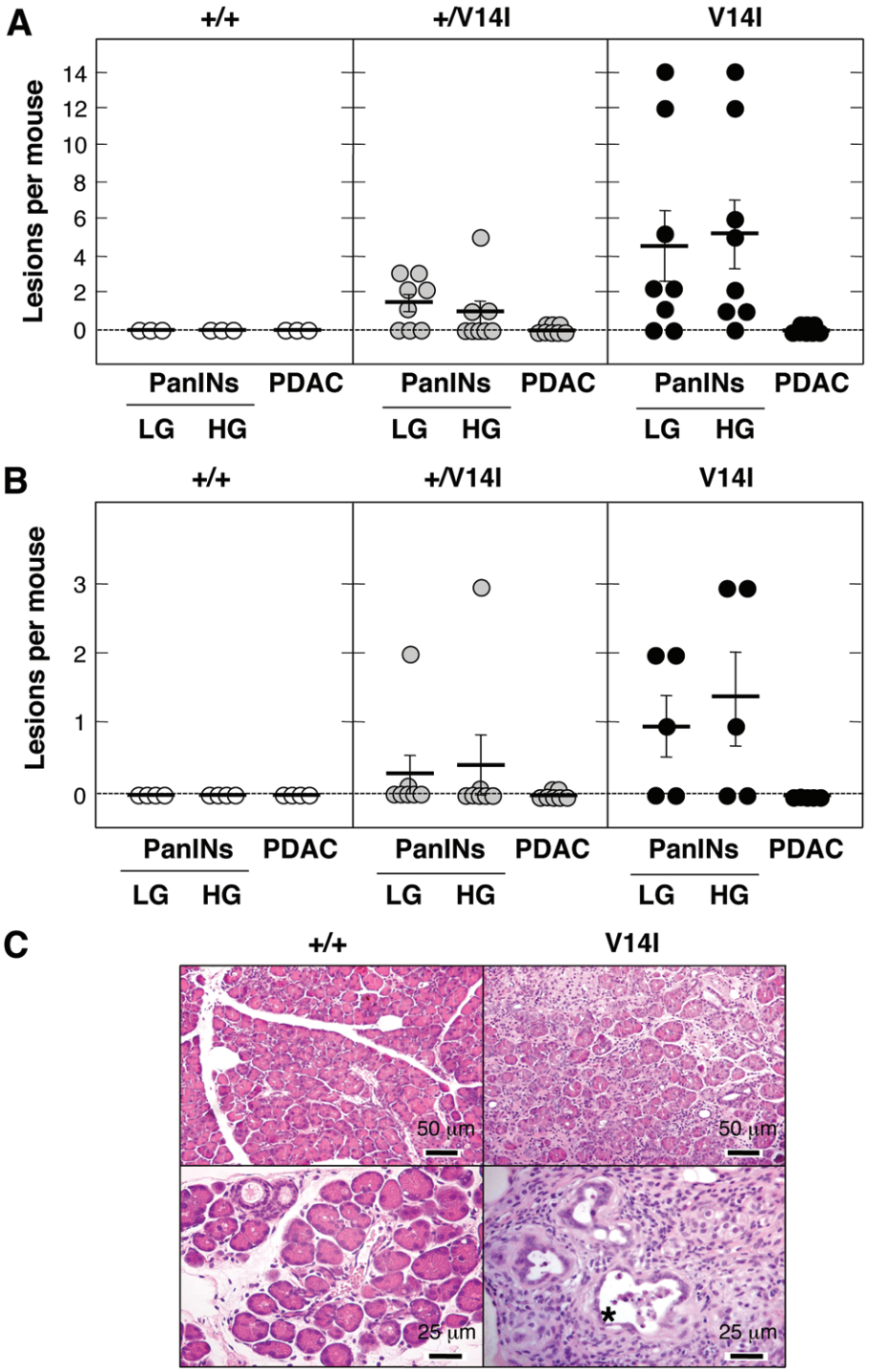

Figure 3. K-*Ras*^{V14I} expression induces PanIN lesions in the context of pancreatitis. (A) Number of low- (LG) and high-grade (HG) PanINs and PDACs per mouse in wild-type (+/+), K-*Ras*$^{+/V14I}$ (+/V14I), and K-*Ras*^{V14I} (V14I) mice. Mice were exposed to caerulein at P60 for 6 months and sacrificed just after treatment. Horizontal bars indicate the average number of lesions per mouse. (B) Number of LG and HG PanINs and PDACs per mouse in wild-type (+/+), K-*Ras*$^{+/V14I}$ (+/V14I), and K-*Ras*^{V14I} (V14I) mice. Mice were exposed to caerulein at P60 for 6 months and sacrificed 3 months after treatment. Horizontal bars indicate the average number of lesions per mouse. (C) H&E-stained paraffin sections of the pancreas of wild-type (+/+) and K-*Ras*^{V14I} (V14I) mice treated with caerulein for 6 months and sacrificed just after treatment. Asterisk indicates a PanIN3 lesion.

p16Ink4a/p19Arf and *Trp53* tumour suppressor genes. *p16Ink4a/p19Arf*-deficient mice develop spontaneous tumours at an early age, including lymphomas and sarcomas, mainly fibrosarcomas [18]. Ablation of *p16Ink4a/p19Arf* in K-*Ras*^{V14I} mice, but not in K-*Ras*$^{+/V14I}$ littermates, led to a 15% lifespan reduction (Figure 5A), which could be attributed to the faster development of haematopoietic malignancies, mainly lymphomas (3/8 mice) and histiocytic sarcomas (7/8 mice), spreading to different organs (Figure 5B, Supplementary Figures 4A and 4B, and Supplementary Table 6). Although these are

Copyright © 2016 Pathological Society of Great Britain and Ireland.
Published by John Wiley & Sons, Ltd. www.pathsoc.org

10969896, 2016, 2, Downloaded from https://pathsocjournals.onlinelibrary.wiley.com/doi/10.1002/path.4719 by Fundacion Del Sector Publico, Wiley Online Library on [19/06/2024]. See the Terms and Conditions (https://onlinelibrary.wiley.com/terms-and-conditions) on Wiley Online Library for rules of use; OA articles are governed by the applicable Creative Commons License

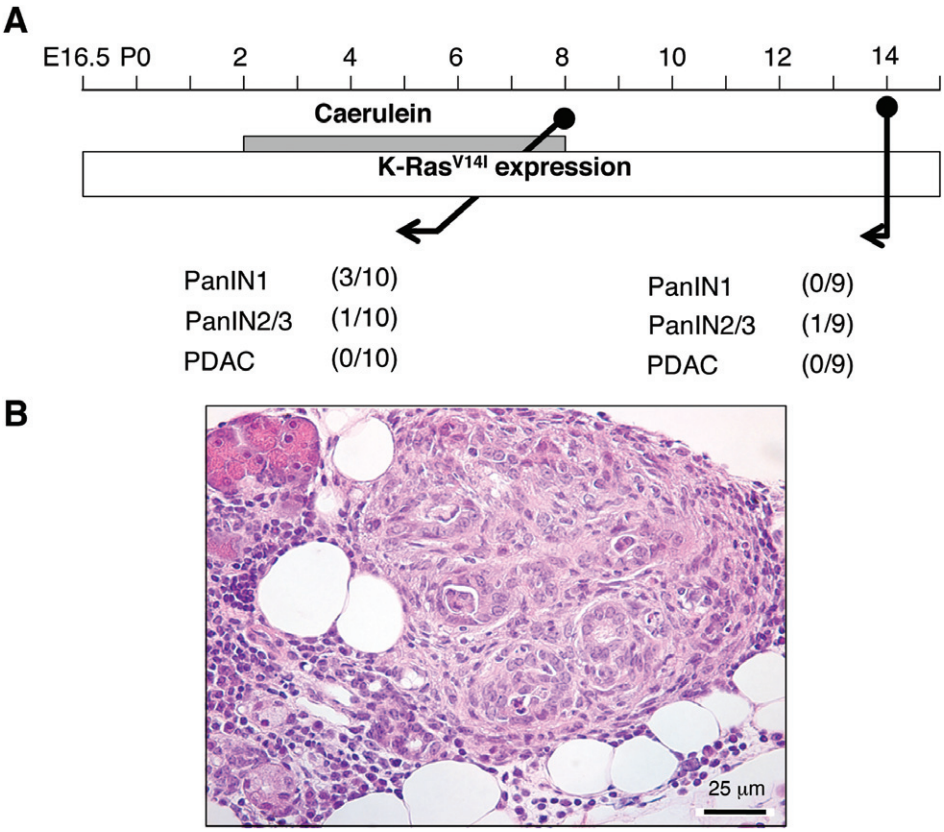

Figure 4. K-*Ras*^{V14I} expression in acinar cells induces a low number of PanIN lesions in the context of pancreatitis. (A) K-*Ras*$^{+/LSLV14I}$;*Elas*-tTA/*tetO*-Cre mice were exposed to caerulein (grey box) for 6 months. The open box indicates the time of the K-*Ras*^{V14I} expression. The number of animals positive for low-grade PanIN1, high-grade PanIN2/3 lesions, and PDAC is indicated for each time point. (B) H&E-stained paraffin sections of the pancreas of K-*Ras*$^{+/LSLV14I}$;*Elas*-tTA/*tetO*-Cre mice treated with caerulein for 6 months and sacrificed 6 months after the end of treatment illustrating a PanIN3.

characteristic tumours of *p16Ink4a/p19Arf*-deficient mice [18], the incidence was significantly different since histiocytic sarcomas have only been observed in around 10% of *p16Ink4a/p19Arf*-deficient mice [18]. This is a very low percentage compared with K-*Ras*^{V14I};*p16Ink4a/p19Arf*$^{-/-}$ mice (87%; 7/8 mice). Interestingly, no fibrosarcomas were found in K-*Ras*^{V14I};*p16Ink4a/p19Arf*$^{-/-}$ mice. Therefore, these results suggest that the elimination of *p16Ink4a/p19Arf* in mice that express two copies of the K-*Ras*^{V14I} mutation promotes the development of haematological abnormalities, preferentially histiocytic sarcomas rather than mesenchymal tumours, such as fibrosarcomas.

Moreover, the K-*Ras*^{V14I} mutation also cooperated with the loss of *Trp53*. K-*Ras*$^{+/V14I}$;*Trp53*$^{-/-}$ mice ($n = 27$) died significantly earlier than *Trp53*$^{-/-}$ animals ($n = 9$) (Figure 5A). *Trp53*-deficient mice spontaneously develop neoplasms at 6 months of age, including lymphomas and sarcomas [19]. The reduction in the lifespan of K-*Ras*$^{+/V14I}$;*Trp53*$^{-/-}$ mice was due to an increase in the number and in the aggressiveness of the tumours previously described in *Trp53*$^{-/-}$ animals (Figure 5C and Supplementary Table 7) [19]; lymphomas spread to more organs (Figure 5C) and angiosarcomas were multicentric (Supplementary Figure 5). Furthermore, most of the mice (7/10) were affected by more than one tumour.

Thus far, we have not been able to obtain K-*Ras*^{V14I};*Trp53*$^{-/-}$ mice, suggesting that the increased dosage effect of the K-*Ras*^{V14I} allele in a *Trp53 null* background may lead to embryonic lethality (Supplementary Table 8).

Loss of heterozygosity (LOH) at the wild-type locus in K-*Ras*^{V14I} mice

Loss of wild-type *Ras* alleles has been observed in aggressive tumours and wild-type *Ras* has been proposed to function as a tumour suppressor [36–38]. Although we were not able to detect LOH in the tumours of K-*Ras*$^{+/V14I}$ mice by laser capture microdissection of tumour cells (Supplementary Figure 6), we addressed whether the elimination of the wild-type allele has a potential role in the development of any K-*Ras*^{V14I}-driven malignancies. Hence, we crossed the K-*Ras*$^{+/V14I}$ mice with heterozygous K-*Ras*$^{+/-}$-deficient mice. Hemizygous B6/129-K-*Ras*$^{V14I/-}$ mice ($n = 14$) were born at the expected Mendelian ratio. At 4 months of age, they displayed an enlarged heart and splenomegaly, mimicking the phenotype of K-*Ras*^{V14I} mice (data not shown) [15]. Moreover, K-*Ras*$^{V14I/-}$ mice ($n = 29$) displayed a similar survival rate to K-*Ras*$^{+/V14I}$ mice (Figure 6). Therefore, the elimination of the wild-type allele did not significantly affect the

Copyright © 2016 Pathological Society of Great Britain and Ireland.
Published by John Wiley & Sons, Ltd. www.pathsoc.org

10969896, 2016, 2, Downloaded from https://pathsocjournals.onlinelibrary.wiley.com/doi/10.1002/path.4719 by Fundacion Del Sector Publico, Wiley Online Library on [19/06/2024]. See the Terms and Conditions (https://onlinelibrary.wiley.com/terms-and-conditions) on Wiley Online Library for rules of use; OA articles are governed by the applicable Creative Commons License

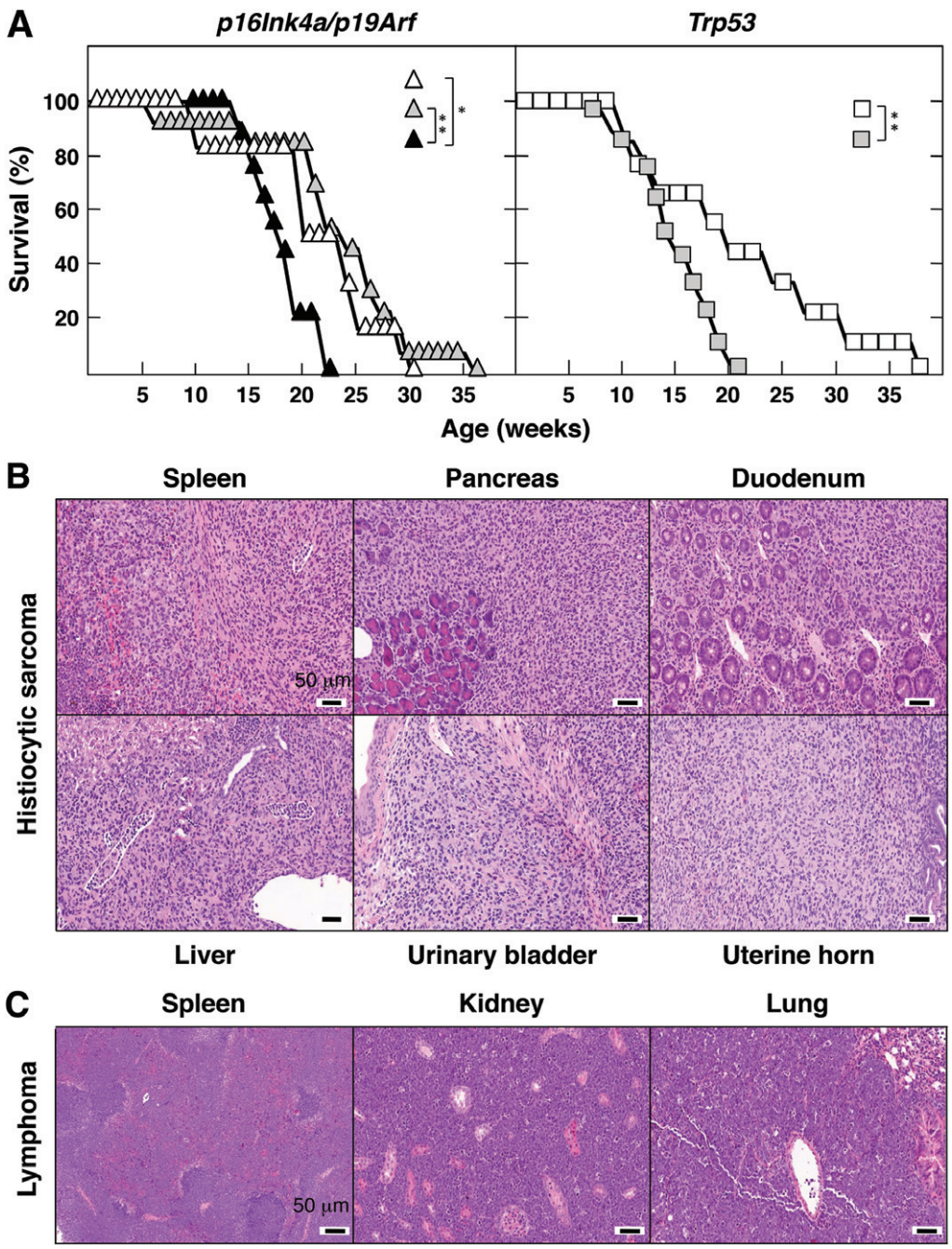

Figure 5. K-*Ras*^{V14I} cooperates with the loss of tumour suppressor genes. (A) Left: survival curve of K-*Ras*$^{+/+}$;*p16Ink4a/p19Arf*$^{-/-}$ ($n=6$; open triangles), K-*Ras*$^{+/V14I}$;*p16Ink4a/p19Arf*$^{-/-}$ ($n=13$; grey triangles), and K-*Ras*^{V14I};*p16Ink4a/p19Arf*$^{-/-}$ mice ($n=9$; black triangles). Right: survival curve of K-*Ras*$^{+/+}$;*Trp53*$^{-/-}$ ($n=9$; open squares) and K-*Ras*$^{+/V14I}$;*Trp53*$^{-/-}$ mice ($n=27$; grey squares). Statistics were calculated using the log-rank (Mantel-Cox) test. $^{*}p<0.1$; $^{**}p<0.01$. (B) Histiocytic sarcoma from a K-*Ras*$^{+/V14I}$;*p16Inka/p19Arf*$^{-/-}$ mouse. H&E-stained paraffin sections of the spleen, pancreas, duodenum, liver, urinary bladder, and uterine horn. (C) Lymphoma from a K-*Ras*$^{+/V14I}$;*Trp53*$^{-/-}$ mouse. H&E-stained sections of the spleen, kidney, and lung.

progression of MPDs (Figure 6). Histological characterization of eight animals at humane endpoints revealed the presence of the same malignancies as those found in K-*Ras*^{V14I} mice: lymphomas (50%), histiocytic sarcomas (38%), and lung adenocarcinomas (12.5%) (Supplementary Table 9). Our results suggest that the loss of the wild-type K-*Ras* allele is not required for the development or the progression of the haematological disorders and it is not sufficient to induce any other kind of tumours.

Discussion

Since RASopathies are disorders that result from germline mutation of genes that encode components or modulators of the RAS/MAPK pathway, which is highly involved in tumour development, it is conceivable to think that these patients might display an increased cancer risk. In the case of NS, there is not enough clinical or epidemiological data to rule out this hypothesis. Only four studies have suggested a small increased risk

Copyright © 2016 Pathological Society of Great Britain and Ireland.
Published by John Wiley & Sons, Ltd. www.pathsoc.org

10969896, 2016, 2, Downloaded from https://pathsocjournals.onlinelibrary.wiley.com/doi/10.1002/path.4719 by Fundacion Del Sector Publico, Wiley Online Library on [19/06/2024]. See the Terms and Conditions (https://onlinelibrary.wiley.com/terms-and-conditions) on Wiley Online Library for rules of use; OA articles are governed by the applicable Creative Commons License

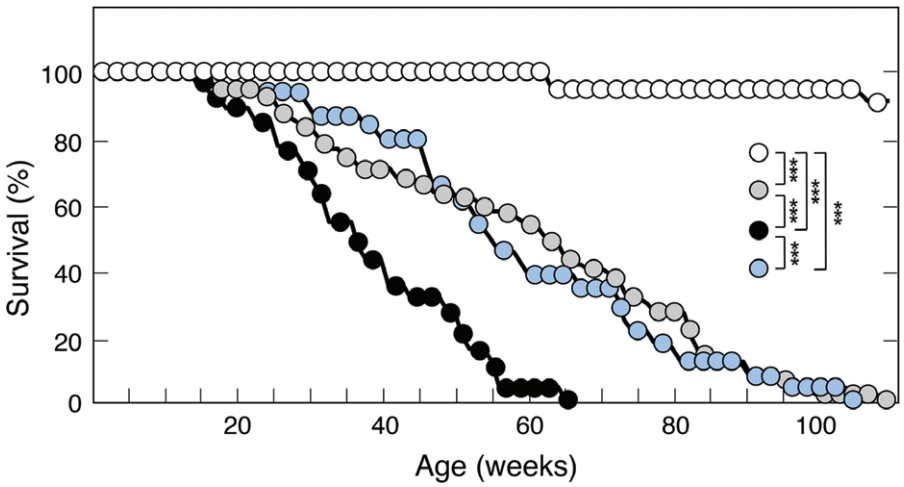

Figure 6. Loss of the wild-type copy of K-*Ras* has no effect on the survival rate. Survival curve of wild-type ($n = 25$; open circles), K-$Ras^{+/V14}$ ($n = 68$; grey circles), K-Ras^{V14I} ($n = 30$; black circles), and K-$Ras^{V14I/-}$ mice ($n = 29$; blue circles). Statistics were calculated using the log-rank (Mantel-Cox) test. ***$p < 0.001$.

of cancer in NS patients, but the underlying molecular mechanisms are currently unknown [11–14].

Interestingly, less than 5% of NS patients carry mutations in the *KRAS* gene [1], but they display lower activation of the MAPK pathway than the classical oncogenic *KRAS* mutations [2]. *KRAS*/NS mutations have intermediate GTPase activity and intermediate levels of GTP hydrolysis in response to GAP-related domains compared with the wild-type and the oncogenic forms [39–41].

Currently, the oncogenic potential of the *KRAS*/NS-associated mutations is unknown. The COSMIC database (http://www.sanger.ac.uk/genetics/CGP/cosmic) reveals $KRAS^{V14I}$ mutations in 20 human tumours (13 colon carcinomas, two pancreatic tumours, two lymphoid neoplasms, one haematopoietic neoplasm, one lung carcinoma, and one endometrial carcinoma). According to the NSEuroNet database (http://www.nseuronet.com), at least 23 KRAS amino acid substitutions, affecting 17 codons, have been identified in NS patients. Among them, 17 *KRAS* mutations have been found in human cancers in the colon, haematopoietic system, lung, pancreas, peritoneum, and liver. Ten mutations have been found exclusively in NS patients (Q22L, N26I, P34Q, P34R, G60S, Y71D, M72L, N85S, N116S, and V152G). While mutations in codons 22, 34, 60, 71, and 72 have been identified in cancer, mutations in codons 26, 85, 116, and 152 remain exclusive to NS patients. Besides, no mutations in codon 61, frequently mutated in cancer, have been found in NS patients so far.

We examined in mice the oncogenic potential of the K-Ras^{V14I} mutation, one of the most frequent in NS patients [42]. Our study provides the first evidence showing that K-Ras^{V14I} expression is associated with an increased risk of tumour development. K-$Ras^{+/V14I}$ and K-Ras^{V14I} mice present with reduced longevity mainly due to the development of haematopoietic alterations. These alterations were developed in combination with MPDs. Similar results were found in mice that express the oncogenic N-Ras^{G12D} mutation in the haematopoietic compartment, which developed an indolent MPD at 6 months of age, which in some mice became fatal. The rest of the N-Ras^{G12D} mice succumbed due to other haematological cancers, including a disorder reminiscent of human myelodysplastic syndrome, lymphoid expansion or lymphoproliferation and histiocytic sarcomas [43].

In the three genetic backgrounds studied (B6/129, 129, and B6), the reduced longevity was linked to splenomegaly and leucocytosis. Interestingly, B6-K-Ras^{V14I} mice preferentially developed lymphomas and histiocytic sarcomas, while 129-K-Ras^{V14I} mice, which displayed a longer survival, were preferentially affected by a severe multifocal perivascular mixed inflammatory reaction. The presence of acute inflammatory areas and vasculitis, suggesting autoimmune problems, was mostly linked to a 129 background. Autoimmune disorders, such as lupus erythematosus, have already been described in NS patients [44]. A prospective study also revealed a two- to three-fold increased risk of autoimmune diseases in *PTPN11*/NS patients [22].

Curiously, some K-Ras^{V14I} mice also developed adenomas and adenocarcinomas in the intestine, liver, and lung. These lesions were only found in the K-$Ras^{+/V14I}$ mice, likely due to their longer survival, but their incidence was very low compared with mice expressing the classical K-*Ras* oncogenes from adulthood, which developed multiple lung and pancreatic tumours with a complete penetrance [16,17,24–26].

Here, we have demonstrated that in contrast to the K-Ras^{G12D} or K-Ras^{G12V} mouse models [16,24–26], mice that express the K-Ras^{V14I} mutation at postnatal stages, either in all cells or only in the lungs, did not develop tumours. Moreover, no other solid tumours were found when the K-Ras^{V14I} mutation was expressed from adult stages in all cells. These results suggest that K-Ras^{V14I} does not have enough oncogenic

Copyright © 2016 Pathological Society of Great Britain and Ireland.
Published by John Wiley & Sons, Ltd. www.pathsoc.org

10969896, 2016, 2, Downloaded from https://pathsocjournals.onlinelibrary.wiley.com/doi/10.1002/path.4719 by Fundacion Del Sector Publico, Wiley Online Library on [19/06/2024]. See the Terms and Conditions (https://onlinelibrary.wiley.com/terms-and-conditions) on Wiley Online Library for rules of use; OA articles are governed by the applicable Creative Commons License

potential. Since adult pancreas seems to be resistant to K-*Ras*^{G12V} oncogenic transformation [17], it was not surprising that K-*Ras*^{V14I} expression from adult stages only induced pancreatic lesions in one 129-K-*Ras*$^{+/V14I}$ mouse. However, as for the oncogenic K-*Ras* mutations [17], K-*Ras*^{V14I} cooperated with chronic pancreatitis to induce preneoplastic lesions. This cooperation was found either when the mutation was expressed through the germline, affecting all pancreatic cells, or only in 20–30% of acinar cells using the conditional pancreatic mouse model. The percentage of LG and HG PanIN lesions was higher in the germline model, likely due to the expression of this mutation in the entire pancreas. In contrast to the oncogenic mutations [17,32], no PDAC lesions were developed upon expression of the K-*Ras*^{V14I} mutation, maybe due to the lower oncogenic capacity of the K-*Ras*^{V14I} mutation.

K-*Ras* oncogenes cooperate with *p16Ink4a/p19Arf* [34,45,46] and *Trp53* tumour suppressor genes [17,26,47,48]. We found that the K-*Ras*^{V14I} mutation cooperated with loss of *p16Ink4a/p19Arf* and *Trp53* genes. Germline expression of two copies of the K-*Ras*^{V14I} mutation significantly accelerated tumour development in mice lacking the *p16Ink4a/p19Arf* genes, resulting in reduced survival. Although these mice developed the typical tumours described for the *p16Ink4a/p19Arf* loss, the incidence of histiocytic sarcomas was greater in K-*Ras*^{V14I};*p16Ink4a/p19Arf*$^{-/-}$ mice than in *p16Ink4a/p19Arf*$^{-/-}$ mice [18]. In contrast to published results [18], we did not find mesenchymal tumours such as fibrosarcomas, which might be explained by genetic background differences. Although K-*Ras* oncogenes and *p16Ink4a/p19Arf* loss cooperate, accelerating PDAC and lung tumour development in mouse models [34,45,46], no other tumours were found in K-*Ras*^{V14I};*p16Ink4a/p19Arf*$^{-/-}$ mice.

Germline expression of the K-*Ras*^{V14I} mutation also accelerated tumour development in mice lacking the *Trp53* tumour suppressor gene. K-*Ras*$^{+/V14I}$;*Trp53*$^{-/-}$ mice died significantly earlier than *Trp53*$^{-/-}$ mice, due to the development of more aggressive tumours. Although these mice developed the typical tumours described for the *Trp53*-null mice [19], they developed faster and were multifocal. Co-existence with different tumour types was also frequently observed. Cooperation between *Trp53* deficiency and the K-*Ras*^{G12D} oncogene expressed by spontaneous recombination reduced longevity, mostly due to the development of aggressive lung tumours, thymic lymphomas, haemangiosarcomas, and fibrosarcomas [26]. This cooperation, in embryonic or adult acinar cells, reduced longevity due to a fast PDAC development [17,48]. In addition, *Trp53* loss promoted the progression of K-*Ras*^{G12D}-induced lung adenocarcinomas [47]. However, we did not detect lung or PDAC tumours in K-*Ras*$^{+/V14I}$;*Trp53*$^{-/-}$ mice, maybe due to the faster development of tumours that resulted in early lethality. Studies with a conditional *Trp53* knock-out mouse should help to clarify this issue.

Finally, *RAS* wild-type alleles are considered tumour suppressors since allelic loss of the wild-type *KRAS* allele (LOH) is found in most human lung adenocarcinomas with *KRAS* oncogenic mutations [49]. Experimentally, it has been observed that the LOH enhances K-*Ras* oncogene-induced lung tumourigenesis [38,50]. Furthermore, LOH of the *HRAS* allele in tumours of some CS patients has also been described [51]. In CS mice, LOH was also described in some papillomas [52]. However, we did not obtain any alteration of the phenotype by elimination of the wild-type H-*Ras* allele in our CS strain (ref 53 and unpublished data). Similarly, our studies did not show cooperation between the loss of the wild-type K-*Ras* allele and the expression of K-*Ras*^{V14I}. K-*Ras*$^{V14I/-}$ mice and K-*Ras*$^{+/V14I}$ mice displayed the same latency, progression, tumour pattern, and survival. So far, there have been no reports illustrating the presence of LOH in NS patients. In agreement, we did not detect LOH in the tumours of the K-*Ras*$^{+/V14I}$ mice.

lAlthough K-*Ras*^{V14I} can be considered a weak oncogene, this mutation confers a higher tumour development risk, yet the low incidence of lung tumours in these mice was unexpected. However, we cannot rule out that non-genetic events could cooperate with the K-*Ras*^{V14I} mutation in lung tumour development, as occurs for the pancreas in the context of pancreatitis. Hence, in view of these results, more studies are needed to learn about the specific tumour development risk of patients carrying the *KRAS*^{V14I} mutation and other *KRAS*/NS-associated mutations. Mouse models are important tools for these studies, helping to verify the cooperation with other genetic and non-genetic events. Moreover, our results support the need for epidemiological studies with NS patients to learn more about the real cancer risk of different NS mutations.

Acknowledgments

We thank M Barbacid for his advice and support, and I Agudo, I Aragón, R Blasco, N Cabrera, MC González, M Lamparero, P Nogales, M San Román, and R Villar for technical assistance. This work was supported by grants from Instituto de Salud Carlos III (Fondo de Investigación Sanitaria) (PI042124, PI08-1623, and PI11-02529), the Autonomous Community of Madrid Consejería de Sanidad, Comunidad de Madrid (GR/SAL/0349/2004), and Fundación Ramón Areces (FRA 01-09-001). IHP was supported by a PFIS grant from the Instituto de Salud Carlos III and AJS by a Grant for Research, Innovation and Cultural Creation from the Fundación BBVA and Consejería de Educación, Juventud y Deporte of Comunidad de Madrid and the People Programme (Marie Curie Actions) of the European Union's Seventh Framework Programme (FP7/2007-2013) under REA grant agreement n° 291820.

Author contribution statement

IHP and CG designed the research. IHP, AJS, RG-M, and BJ performed the experimental work. MC and AM

Copyright © 2016 Pathological Society of Great Britain and Ireland.
Published by John Wiley & Sons, Ltd. www.pathsoc.org

10969896, 2016, 2, Downloaded from https://pathsocjournals.onlinelibrary.wiley.com/doi/10.1002/path.4719 by Fundacion Del Sector Publico, Wiley Online Library on [19/06/2024]. See the Terms and Conditions (https://onlinelibrary.wiley.com/terms-and-conditions) on Wiley Online Library for rules of use; OA articles are governed by the applicable Creative Commons License

analysed the histological data. IHP, AJS, RG-M, and CG wrote the manuscript and CG obtained funding.

References

1. Schubbert S, Shannon K, Bollag G. Hyperactive Ras in developmental disorders and cancer. *Nature Rev Cancer* 2007; **7:** 295–308.
2. Fernandez-Medarde A, Santos E. Ras in cancer and developmental diseases. *Genes Cancer* 2011; **2:** 344–358.
3. Rauen KA. The RASopathies. *Annu Rev Genomics Hum Genet* 2013; **14:** 355–369.
4. Roberts AE, Allanson JE, Tartaglia M, *et al.* Noonan syndrome. *Lancet* 2013; **381:** 333–342.
5. Aoki Y, Niihori T, Banjo T, *et al.* Gain-of-function mutations in RIT1 cause Noonan syndrome, a RAS/MAPK pathway syndrome. *Am J Hum Genet* 2013; **93:** 173–180.
6. Flex E, Jaiswal M, Pantaleoni F, *et al.* Activating mutations in *RRAS* underlie a phenotype within the RASopathy spectrum and contribute to leukaemogenesis. *Hum Mol Genet* 2014; **23:** 4315–4327.
7. Tartaglia M, Gelb BD, Zenker M. Noonan syndrome and clinically related disorders. *Best Pract Res Clin Endocrinol Metab* 2011; **25:** 161–179.
8. Kwon MC, Berns A. Mouse models for lung cancer. *Mol Oncol* 2013; **7:** 165–177.
9. Gripp KW. Tumor predisposition in Costello syndrome. *Am J Med Genet C Semin Med Genet* 2005; **137C:** 72–77.
10. Niemeyer CM. RAS diseases in children. *Haematologica* 2014; **99:** 1653–1662.
11. Jongmans MC, van der Burgt I, Hoogerbrugge PM, *et al.* Cancer risk in patients with Noonan syndrome carrying a *PTPN11* mutation. *Eur J Hum Genet* 2011; **19:** 870–874.
12. Smpokou P, Zand DJ, Rosenbaum KN, *et al.* Malignancy in Noonan syndrome and related disorders. *Clin Genet* 2015; **88:** 516–522.
13. Kratz CP, Rapisuwon S, Reed H, *et al.* Cancer in Noonan, Costello, cardiofaciocutaneous and LEOPARD syndromes. *Am J Med Genet C Semin Med Genet* 2011; **157C:** 83–89.
14. Kratz CP, Franke L, Peters H, *et al.* Cancer spectrum and frequency among children with Noonan, Costello, and cardio-facio-cutaneous syndromes. *Br J Cancer* 2015; **112:** 1392–1397.
15. Hernandez-Porras I, Fabbiano S, Schuhmacher AJ, *et al.* K-Ras^{V14I} recapitulates Noonan syndrome in mice. *Proc Natl Acad Sci U S A* 2014; **111:**16395–16400.
16. Guerra C, Mijimolle N, Dhawahir A, *et al.* Tumor induction by an endogenous *K-ras* oncogene is highly dependent on cellular context. *Cancer Cell* 2003; **4:** 111–120.
17. Guerra C, Schuhmacher AJ, Canamero M, *et al.* Chronic pancreatitis is essential for induction of pancreatic ductal adenocarcinoma by K-*Ras* oncogenes in adult mice. *Cancer Cell* 2007; **11:** 291–302.
18. Serrano M, Lee H, Chin L, *et al.* Role of the *INK4a* locus in tumor suppression and cell mortality. *Cell* 1996; **85:** 27–37.
19. Donehower LA, Harvey M, Slagle BL, *et al.* Mice deficient for p53 are developmentally normal but susceptible to spontaneous tumours. *Nature* 1992; **356:** 215–221.
20. Simpson AJ, Wallace WA, Marsden ME, *et al.* Adenoviral augmentation of elafin protects the lung against acute injury mediated by activated neutrophils and bacterial infection. *J Immunol* 2001; **167:** 1778–1786.
21. Hernandez-Porras I, Jimenez- Catalan B, Schuhmacher AJ, *et al.* The impact of genetic backgrounds in the K-RasV14I-induced Noonan syndrome. *Rare Diseases* 2015; e1045169.
22. Quaio CR, Carvalho JF, da Silva CA, *et al.* Autoimmune disease and multiple autoantibodies in 42 patients with RASopathies. *Am J Med Genet A* 2012; **158A:** 1077–1082.
23. Forbes SA, Bindal N, Bamford S, *et al.* COSMIC: mining complete cancer genomes in the Catalogue of Somatic Mutations in Cancer. *Nucleic Acids Res* 2011; **39:** D945–D950.
24. Tuveson DA, Shaw AT, Willis NA, *et al.* Endogenous oncogenic *K-ras^{G12D}* stimulates proliferation and widespread neoplastic and developmental defects. *Cancer Cell* 2004; **5:** 375–387.
25. Jackson EL, Willis N, Mercer K, *et al.* Analysis of lung tumor initiation and progression using conditional expression of oncogenic *K-ras*. *Genes Dev* 2001; **15:** 3243–3248.
26. Johnson L, Mercer K, Greenbaum D, *et al.* Somatic activation of the *K-ras* oncogene causes early onset lung cancer in mice. *Nature* 2001; **410:** 1111–1116.
27. Mainardi S, Mijimolle N, Francoz S, *et al.* Identification of cancer initiating cells in *K-Ras* driven lung adenocarcinoma. *Proc Natl Acad Sci U S A* 2013; **111:** 255–260.
28. Almoguera C, Shibata D, Forrester K, *et al.* Most human carcinomas of the exocrine pancreas contain mutant c-K-*ras* genes. *Cell* 1988; **53:** 549–554.
29. Hezel AF, Kimmelman AC, Stanger BZ, *et al.* Genetics and biology of pancreatic ductal adenocarcinoma. *Genes Dev* 2006; **20:** 1218–1249.
30. Siegel R, Naishadham D, Jemal A. Cancer statistics, 2013. *CA Cancer J Clin* 2013; **63:** 11–30.
31. Guerra C, Barbacid M. Genetically engineered mouse models of pancreatic adenocarcinoma. *Mol Oncol* 2013; **7:** 232–247.
32. Hingorani SR, Petricoin EF, Maitra A, *et al.* Preinvasive and invasive ductal pancreatic cancer and its early detection in the mouse. *Cancer Cell* 2003; **4:** 437–450.
33. Malka D, Hammel P, Maire F, *et al.* Risk of pancreatic adenocarcinoma in chronic pancreatitis. *Gut* 2002; **51:** 849–52.
34. Guerra C, Collado M, Navas C, *et al.* Pancreatitis-induced inflammation contributes to pancreatic cancer by inhibiting oncogene-induced senescence. *Cancer Cell* 2011; **19:** 728–739.
35. Maitra A, Hruban RH. Pancreatic cancer. *Annu Rev Pathol* 2008; **3:** 157–188.
36. Zhang Z, Wang Y, Vikis HG, *et al.* Wildtype *Kras2* can inhibit lung carcinogenesis in mice. *Nature Genet* 2001; **29:** 25–33.
37. Diaz R, Ahn D, Lopez-Barcons L, *et al.* The N-*ras* proto-oncogene can suppress the malignant phenotype in the presence or absence of its oncogene. *Cancer Res* 2002; **62:** 4514–4518.
38. Grabocka E, Pylayeva-Gupta Y, Jones MJ, *et al.* Wild-type H- and N-Ras promote mutant K-Ras-driven tumorigenesis by modulating the DNA damage response. *Cancer Cell* 2014; **25:** 243–256.
39. Gremer L, Merbitz-Zahradnik T, Dvorsky R, *et al.* Germline *KRAS* mutations cause aberrant biochemical and physical properties leading to developmental disorders. *Hum Mutat* 2011; **32:** 33–43.
40. Schubbert S, Zenker M, Rowe SL, *et al.* Germline *KRAS* mutations cause Noonan syndrome. *Nature Genet* 2006; **38:** 331–336.
41. Schubbert S, Bollag G, Lyubynska N, *et al.* Biochemical and functional characterization of germ line *KRAS* mutations. *Mol Cell Biol* 2007; **27:** 7765–7770.
42. Lo FS, Lin JL, Kuo MT, *et al.* Noonan syndrome caused by germline *KRAS* mutation in Taiwan: report of two patients and a review of the literature. *Eur J Pediatr* 2009; **168:** 919–923.
43. Li Q, Haigis KM, McDaniel A, *et al.* Hematopoiesis and leukemogenesis in mice expressing oncogenic *Nras^{G12D}* from the endogenous locus. *Blood* 2011; **117:** 2022–2032.
44. Leventopoulos G, Denayer E, Makrythanasis P, *et al.* Noonan syndrome and systemic lupus erythematosus in a patient with a novel *KRAS* mutation. *Clin Exp Rheumatol* 2010; **28:** 556–557.
45. Aguirre AJ, Bardeesy N, Sinha M, *et al.* Activated Kras and *Ink4a/Arf* deficiency cooperate to produce metastatic pancreatic ductal adenocarcinoma. *Genes Dev* 2003; **17:** 3112–3126.

Copyright © 2016 Pathological Society of Great Britain and Ireland.
Published by John Wiley & Sons, Ltd. www.pathsoc.org

10969896, 2016, 2, Downloaded from https://pathsocjournals.onlinelibrary.wiley.com/doi/10.1002/path.4719 by Fundacion Del Sector Publico, Wiley Online Library on [19/06/2024]. See the Terms and Conditions (https://onlinelibrary.wiley.com/terms-and-conditions) on Wiley Online Library for rules of use; OA articles are governed by the applicable Creative Commons License

46. Ji H, Ramsey MR, Hayes DN, *et al.* LKB1 modulates lung cancer differentiation and metastasis. *Nature* 2007; **448:** 807–810.
47. Jackson EL, Olive KP, Tuveson DA, *et al.* The differential effects of mutant p53 alleles on advanced murine lung cancer. *Cancer Res* 2005; **65:** 10280–10288.
48. Hingorani SR, Wang L, Multani AS, *et al.* *Trp53*^{R172H} and *Kras*^{G12D} cooperate to promote chromosomal instability and widely metastatic pancreatic ductal adenocarcinoma in mice. *Cancer Cell* 2005; **7:** 469–483.
49. Li J, Zhang Z, Plass C, *et al.* LOH of chromosome 12p correlates with Kras2 mutation in non-small cell lung cancer. *Oncogene* 2003; **22:** 1243–1246.
50. Puyol M, Martin A, Dubus P, *et al.* A synthetic lethal interaction between K-Ras oncogenes and Cdk4 unveils a therapeutic strategy for non-small cell lung carcinoma. *Cancer Cell* 2010; **18:** 63–73.
51. Estep AL, Tidyman WE, Teitell MA, *et al.* *HRAS* mutations in Costello syndrome: detection of constitutional activating mutations in codon 12 and 13 and loss of wild-type allele in malignancy. *Am J Med Genet A* 2006; **140:** 8–16.
52. Chen X, Mitsutake N, LaPerle K, *et al.* Endogenous expression of Hras^{G12V} induces developmental defects and neoplasms with copy number imbalances of the oncogene. *Proc Natl Acad Sci U S A* 2009; **106:** 7979–7984.
53. Schuhmacher AJ, Guerra C, Sauzeau V, *et al.* A mouse model for Costello syndrome reveals an Ang II-mediated hypertensive condition. *J Clin Invest* 2008; **118:** 2169–2179.

SUPPORTING INFORMATION ON THE INTERNET

The following supporting information may be found in the online version of this article:

Figure S1. B6/129-K-*Ras*^{V14I} mice develop renal pathological alterations and vasculitis.

Figure S2. 129-K-*Ras*^{V14I} mice develop an acute inflammatory reaction and vasculitis.

Figure S3. K-*Ras*^{V14I} expression induces PanIN lesions in the context of pancreatitis.

Figure S4. K-*Ras*^{V14I};*p16Ink4a/p19Arf*$^{-/-}$ mice develop histiocytic sarcomas and B-cell lymphomas.

Figure S5. K-*Ras*^{V14I};*Trp53*$^{-/-}$ mice develop lymphomas and angiosarcomas.

Figure S6. The wild-type K-*Ras*$^{+}$ allele is maintained in K-*Ras*$^{+/V14I}$ tumours.

Table S1. Summary of the pathological alterations found in B6/129 mice.

Table S2. Summary of the pathological alterations found in B6/129 K-*Ras*$^{+/V14I}$ and K-*Ras*^{V14I} mice sacrificed at humane endpoint.

Table S3. Summary of the pathological alterations found in K-*Ras*$^{+/+}$ mice.

Table S4. Description of the pathological alterations found in B6- and 129-K-*Ras*^{V14I} mice.

Table S5. Summary of the pathological alterations found in B6- and 129-K-*Ras*^{V14I} mice.

Table S6. Summary of the tumours observed in K-*Ras*^{V14I};*p16Ink4a/p19Arf*$^{-/-}$ and K-*Ras*$^{+/V14I}$;*p16Ink4a/p19Arf*$^{-/-}$mice.

Table S7. Summary of the tumours observed in the K-*Ras*$^{+/V14I}$;*Trp53*$^{-/-}$ mice.

Table S8. Offspring from matings between K-*Ras*$^{+/V14I}$;*Trp53*$^{-/-}$ and K-*Ras*$^{+/V14I}$;*Trp53*$^{+/-}$ mice.

Table S9. Summary of the pathological alterations observed in K-*Ras*$^{V14I/-}$ mice.

25 Years ago in the *Journal of Pathology…*

Cell adhesion and epithelial differentiation

Stewart Fleming

To view these articles, and more, please visit: www.thejournalofpathology.com

Click 'ALL ISSUES (1892 - 2016)', to read articles going right back to Volume 1, Issue 1.

The Journal of Pathology
Understanding Disease

A Journal of The Pathological Society

Copyright © 2016 Pathological Society of Great Britain and Ireland.
Published by John Wiley & Sons, Ltd. www.pathsoc.org

10969896, 2016, 2, Downloaded from https://pathsocjournals.onlinelibrary.wiley.com/doi/10.1002/path.4719 by Fundacion Del Sector Publico, Wiley Online Library on [19/06/2024]. See the Terms and Conditions (https://onlinelibrary.wiley.com/terms-and-conditions) on Wiley Online Library for rules of use; OA articles are governed by the applicable Creative Commons License